Functional recovery and muscle atrophy in pre-clinical models of peripheral nerve transection and gap-grafting in mice: effects of 4-aminopyridine

Jung Il Lee[1, 2], M A Hassan Talukder[1, *], Zara Karuman[1], Anagha A. Gurjar[1], Prem Kumar Govindappa[1], Jagadeeshaprasad M. Guddadarangaiah[1], Kristen M. Manto[1], Grant D. Wandling[1], John P. Hegarty[1], David L. Waning[3], John C. Elfar[1, *]

https://doi.org/10.4103/1673-5374.346456

Date of submission: June 3, 2021

Date of decision: September 8, 2021

Date of acceptance: April 22, 2022

Date of web publication: June 2, 2022

From the Contents

Graphical Abstract

Differential effects of 4-aminopyridine (4-AP) on functional recovery and muscle atrophy in mouse models of peripheral nerve injury (PNI) and repair

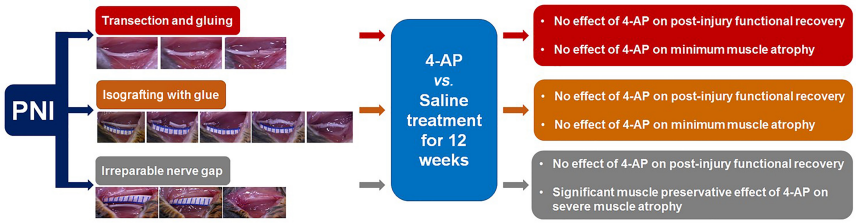

Abstract

We recently demonstrated a repurposing beneficial effect of 4-aminopyridine (4-AP), a potassium channel blocker, on functional recovery and muscle atrophy after sciatic nerve crush injury in rodents. However, this effect of 4-AP is unknown in nerve transection, gap, and grafting models. To evaluate and compare the functional recovery, nerve morphology, and muscle atrophy, we used a novel stepwise nerve transection with gluing (STG), as well as 7-mm irreparable nerve gap (G-7/0) and 7-mm isografting in 5-mm gap (G-5/7) models in the absence and presence of 4-AP treatment. Following surgery, sciatic functional index was determined weekly to evaluate the direct *in vivo* global motor functional recovery. After 12 weeks, nerves were processed for whole-mount immunofluorescence imaging, and tibialis anterior muscles were harvested for wet weight and quantitative histomorphological analyses for muscle fiber cross-sectional area and minimal Feret's diameter. Average post-injury sciatic functional index values in STG and G-5/7 models were significantly greater than those in the G-7/0 model. 4-AP did not affect the sciatic functional index recovery in any model. Compared to STG, nerve imaging revealed more misdirected axons and distorted nerve architecture with isografting. While muscle weight, cross-sectional area, and minimal Feret's diameter were significantly smaller in G-7/0 model compared with STG and G-5/7, 4-AP treatment significantly increased right TA muscle mass, cross-sectional area, and minimal Feret's diameter in G-7/0 model. These findings demonstrate that functional recovery and muscle atrophy after peripheral nerve injury are directly related to the intervening nerve gap, and 4-AP exerts differential effects on functional recovery and muscle atrophy.

Key Words: 4-aminopyridine; functional recovery; muscle atrophy; nerve gap; nerve grafting; nerve imaging; nerve transection

Introduction

Peripheral nerve injury (PNI) is a major clinical and public health problem costing billions of dollars annually (Noble et al., 1998; Robinson, 2000; Foster et al., 2019; Karsy et al., 2019). PNI can occur from injuries in which some axonal continuity is maintained and injuries where the nerve is completely transected with an intervening gap (Robinson, 2004; Campbell, 2008; Menorca et al., 2013). The key consequence of PNI is poor functional recovery and denervation-induced muscle loss (Engel and Stonnington, 1974; Day et al., 2001; Lien et al., 2008; Wong and Pomerantz, 2019), which predispose to permanent disability. The treatment of choice for nerve transection injury is end-to-end repair with tensionless epineurial sutures or nerve grafting, nerve conduits, or nerve transfer if the end-to-end anastomosis is not possible (Siemionow and Brzezicki, 2009; Isaacs, 2013). Despite these advanced microsurgical techniques, the functional outcomes after nerve repair and grafting are poor (Zochodne, 2012; Faroni et al., 2015), and full functional recovery is rare.

While it is not possible to investigate the mechanisms of poor functional outcomes in humans, we developed a novel standardized peripheral nerve transection technique which we refer to as stepwise transection and fibrin glue (STG) in mice (Lee et al., 2020). Our STG method demonstrated a close resemblance to the pathophysiological characteristics of nerve transection with gold-standard epineural suturing. However, the situation is different with a transection injury where two ends of the severed nerve are separated by a large intervening gap, and the impact of nerve grafting of irreparable nerve gaps with fibrin gluing remains poorly characterized for functional recovery and muscle atrophy.

Although no medical treatment exists for PNI, several pharmacological agents and rehabilitation strategies have been reported to enhance functional recovery in preclinical studies (Martínez de Albornoz et al., 2011; Udina et al., 2011; Isaacs, 2013; Chan et al., 2014; Fernandez et al., 2018; Hussain et al., 2020; Modrak et al., 2020). Among the pharmacological agents, erythropoietin, tacrolimus (FK506), steroids, N-acetyl-cysteine, and rolipram, have shown some promise in animal studies (Chan et al., 2014; Fernandez et al., 2018; Modrak et al., 2020); however, they have significant limitations with optimal dosing, timing and duration of treatment, and adverse effects. We have demonstrated a potential repurposing effect of 4-aminopyridine (4-AP), a potent potassium channel blocker and a Food and Drug Administration-

[1]Department of Orthopaedics and Rehabilitation, Center for Orthopaedic Research and Translational Science, The Pennsylvania State University College of Medicine, Hershey, PA, USA; [2]Department of Orthopaedic Surgery, Korea University Guro Hospital, Seoul, South Korea; [3]Department of Cellular and Molecular Physiology, The Pennsylvania State University College of Medicine, Hershey, PA, USA

***Correspondence to:** John C. Elfar, MD, openelfar@gmail.com; M A Hassan Talukder, MD, PhD, mahassanatlaukder@yahoo.com.
https://orcid.org/0000-0002-4438-7118 (John C. Elfar); https://orcid.org/0000-0002-8352-2247 (M A Hassan Talukder)

Funding: *This work was supported by grants from the National Institutes of Health, USA (No. K08 AR060164-01A) and Department of Defense, USA (Nos. W81XWH-16-1-0725 and W81XWH-19-1-0773) in addition to institutional support from the Pennsylvania State University College of Medicine.*

How to cite this article: *Lee JI, Talukder MAH, Karuman Z, Gurjar AA, Govindappa PK, Guddadarangaiah JM, Manto KM, Wandling GD, Hegarty JP, Waning DL, Elfar JC (2023) Functional recovery and muscle atrophy in pre-clinical models of peripheral nerve transection and gap-grafting in mice: effects of 4-aminopyridine. Neural Regen Res 18(2):439-444.*

approved drug for neurodegenerative disorders, on nerve myelination, nerve conduction, neurogenic muscle atrophy, muscle regenerating stem cells, and functional recovery after sciatic nerve crush injury in mice (Tseng et al., 2016; Clark et al., 2019; Noble et al., 2019; Hsu et al., 2020). However, it is unknown whether the beneficial effects of 4-AP in functional recovery and muscle atrophy are present after nerve transection and repair, especially in the setting of the nerve gap.

In this study, we present a novel peripheral nerve gap and grafting model in a series of mice using fibrin glue. The main objective of this study was to evaluate the long-term functional recovery, nerve morphology, and muscle atrophy in nerve transection, gap, and grafting models, and the effects of 4-AP in these models.

Methods

Animals

The experimental animal protocol was approved by the Institutional Animal Care and Use Committee (IACUC) at The Pennsylvania State University College of Medicine (PRAMS201747923) on November 18, 2020. Ninety-six 10-week-old male C57BL/6J mice (Cat# 000664; Jackson Laboratories, Bar Harbor, ME, USA) weighing 20–25 g, were used in this study: Sixty mice (n = 10/group) were used for nerve transection, isografting, and gap models, and thirty-six mice (n = 6/group) were used for the dose effects of 4-AP in severe sciatic nerve crush injury model (see **Additional file 1** for the supplemental methods).

Mouse models of peripheral nerve transection injury and isografting

Briefly, under deep anesthesia with an intraperitoneal injection of ketamine (100 mg/kg) and xylazine (10 mg/kg) mixture (supplied by Animal Care Facility), the mice were prepped and draped in a sterile fashion. A 2-cm long skin incision was made on the extended posterior right hind limb to expose the right sciatic nerve under an operating microscope (Model PZMIII, World Precision Instruments, Sarasota, FL, USA). As described recently for the stepwise transection and fibrin glue (STG) method (Lee et al., 2020) and shown in **Figure 1A**, the nerve was first transected to 80% of its width to prevent gap formation between the cutends, then 10 µL of fibrin glue was applied around the transection site and the nerve was completely transected before complete clotting of fibrin glue. This method effectively standardized gap formation between the transected nerve ends to 1–2 mm while minimizing manipulation of the nerve. In the graded nerve gap and grafting model (**Figure 1B** and **C**), pairs of mice were used in series for cascade syngeneic nerve grafting in 1 set of experiments. In mouse #1, a large gap was created by dissecting out 7 mm (G-7/0) of the right sciatic nerve section. The proximal stump of the sciatic nerve was buried underneath the muscle with 10 µL of fibrin glue. Then, in mouse #2, a medium gap was created by dissecting out 5 mm of the right sciatic nerve section and the 7 mm dissected nerve section from mouse #1 was grafted and kept in good alignment with fibrin glue at both ends (G-5/7). The skin was closed with surgical staples and post-operative slow-release buprenorphine (0.05 mg/kg, supplied by Animal Care Facility) was given subcutaneously to all animals as an analgesic. Animals were monitored on the warming pad until active and then returned to the animal facility under the supervision of the attending veterinarian. Post-injury functional recovery was assessed by walking track analysis (sciatic functional index [SFI]). After 12 weeks of surgery, nerves and muscles were processed for whole-mount imaging and histomorphometric analysis, respectively.

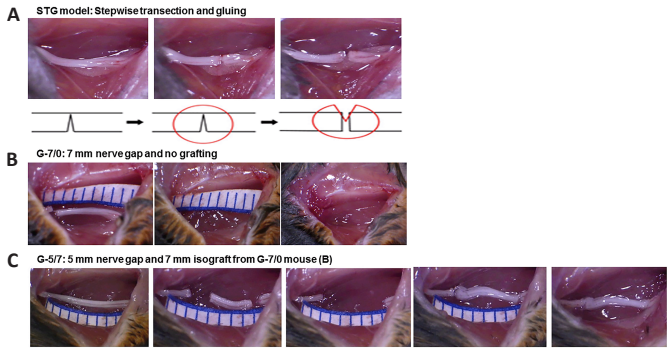

Figure 1 | Surgical steps and gross nerve images in STG and cascade syngeneic nerve grafting.
In STG (A), the nerve was first transected to 80% of its width to prevent gap formation between the cut ends, then 10 µL of fibrin glue was applied around the transection site and the nerve was completely transected before complete clotting of fibrin glue. In G-7/0 (B), a large gap was created by dissecting a 7 mm nerve section from mouse #1. In G-5/7 (C), a medium gap was created by dissecting the 5 mm nerve section and the 7 mm dissected nerve section from the mouse in G-7/0 was grafted and kept in good alignment with fibrin glue. G-5/7: 5 mm gap and 7 mm nerve grafting; G-7/0: 7 mm permanent nerve gap; STG: stepwise transection and fibrin glue.

As shown in **Figure 2**, the experimental animals were randomized using the random number table method immediately after surgery to intraperitoneal normal saline (0.1 mL/mouse) and 4-AP (MilliporeSigma, Burlington, MA, USA; 40 µg/20 g mouse) treatment twice daily for 12 weeks. This body mass-adjusted dose of 4-AP (2 mg/kg) is equivalent to the lowest available starting dose in humans (10 mg daily) (Nair and Jacob, 2016), and twice daily dosing was chosen based on our dose-escalating effect in severe (34 MPa pressure) nerve crush injury model (Supplemental methods [**Additional file 1**] and **Additional Figure 1**).

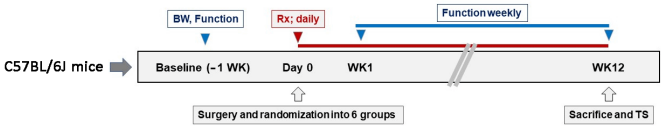

Figure 2 | Experimental timeline/design.
The experimental design was for 12 weeks and 10 C57BL/6J mice were randomly assigned to each group. Experimental groups: STG-Saline; STG-4-AP; G-5/7-Saline; G-5/7-4-AP; G-7/0-Saline; G-7/0- 4-AP. G-5/7: 5 mm gap and 7 mm nerve grafting; G-7/0: 7 mm permanent nerve gap; STG: stepwise transection, and fibrin glue. BW: Body weight (g); Function: walking track analysis for sciatic function index; Treatment (Rx): intraperitoneal saline (100 µL) or 40 µg/20 g twice daily for 12 weeks; TS: tissue sampling for histological and immunohistochemical studies; WK: week or weekly.

Sciatic functional index

To evaluate post-injury global motor function recovery, the sciatic functional index (SFI) was determined in all experimental mice by walking track analysis 1 week before injury (pre-injury baseline) and weekly after surgery for 12 weeks, as previously described (Varejão et al., 2001; Yue et al., 2019). Briefly, mice were trained to walk freely along a wooden corridor lined with white paper and individual footprints of the hind limbs was obtained by painting each foot with ink. At least three measurable footprints for each hind limb were obtained. Two blinded observers selected three footprints per hind limb, which were measured by digital calipers. SFI was calculated using three parameters of footprints: (1) toe spread (TS, first to the fifth toe), (2) total print length (PL), and (3) intermediate toe spread (IT, second to the fourth toe) and the following formula: SFI = –38.3 [(EPL–NPL)/NPL] + 109.5 [(ETS–NTS)/NTS] + 13.3 [(EIT–NIT)/NIT] – 8.8, where E for experimental (injured) and N for normal (contralateral uninjured) sides. The SFI score is expressed on a scale of 0 to –100, where 0 is the baseline SFI and –100 is the worst possible SFI after PNI.

Whole-mount immunostaining of nerves

The whole-mount nerve immunostaining was performed as described (Lee et al., 2020). Briefly, after 12 weeks of surgery, entire left and right sciatic nerves from both saline and 4-AP groups were fixed in 4% paraformaldehyde at 4°C for 5 hours, washed three times 10 minutes each with PTX (phosphate-buffered saline [PBS] with 1% Triton X-100 [CAS 9002-93-1, MilliporeSigma]) and incubated in blocking solution (10% normal goat serum [Jackson Immunoresearch, 005-000-121]) in 5% bovine serum albumin (BSA)-PTX overnight at 4°C. On the next day, nerves were transferred into primary antibodies in 5% bovine serum albumin-PTX and incubated for 72 hours at 4°C with gentle rocking. Primary antibodies for mouse were used to detect neurofilament heavy chain (NF-H) (1:1000; NB300-135, Novus biologicals, Littleton, CO, USA), P-zero Myelin protein (MP0) (1:500; PZ0, Aves Labs, Davis, CA, USA), and endothelial cells (CD31) (1:100; 553370, BD Pharmingen, Bath, UK). For fluorescent detection and visualization of target proteins (primary antibodies), Alexa Fluor secondary antibodies were used. After PTX washes, nerves were incubated with Alexa Fluor 488, 594, and 647-conjugated secondary antibodies (1:500; Invitrogen, Waltham, MA, USA) for 48 hours at 4°C with gentle rocking. Nerves were washed in PTX three times for 15 minutes each, followed by 4-hour washing in PTX with PTX change at every hour. Nerves were then washed overnight without changing PTX at 4°C. The next day, nerves were washed with PBS (three times 10 minutes each) for the removal of triton and cleared sequentially in 25%, 50% glycerol (G6279, MilliporeSigma) in PBS for 6 and 12 hours respectively for each glycerol concentration. Then, nerves were mounted in SlowFade™ Gold Antifade Mountant with DAPI (S36939, Invitrogen) or without DAPI (S36937, Invitrogen). Stained whole nerves were imaged using ZEISS Axio Observer 7 equipped with an Apotome.2 (Carl Zeiss Microscopy GmbH, Jena, Germany). Tiling and Z-stack functions both were employed to image the whole nerve. Maximum Intensity projection was used to pull the data from all Z-stacks and represented as a 2D image.

Hematoxylin and eosin staining and histomorphometric analysis of muscles

After final SFI on post-surgery week 12, tibialis anterior (TA) muscles of both hind limbs were harvested and weighed. H&E staining and histomorphometric analysis of TA muscles were performed as described previously (Yue et al., 2019; Lee et al., 2020). Briefly, four paired TA muscles from healthy (uninjured) left hindlimb and from injured right hindlimb were used for cryosectioning. Three 10 µm thick sections from each muscle were cut at –21°C using a Cryostat (Microm HM505e, Thermo Fisher Scientific, Waltham, MA, USA) and collected on superfrost plus microscopic slides (Fisherbrand, 12-550-15; Fisher Scientific, Hampton, NH, USA). Slides were then stained for hematoxylin and eosin (H&E) and imaged on an Olympus BX53 microscope (Hunt Optics and Imaging, Pittsburgh, PA, USA). Quantitative analysis for cross-sectional area (CSA), minimum Feret's diameter (MFD), and fiber distribution of muscle fiber were done with ImageJ software (version 1.41; NIH, Bethesda, MD, USA; Schneider et al., 2012) on three random microscopic fields from each muscle.

Data analysis

The number of animals (n) needed was based on the conservative use of animals for the least sensitive data type and was determined based on the

desired power level greater than 80% and a significance value of < 0.05. This resulted in *n* = 8–9 animals per group for *in vivo* functional analysis (SFI), with fewer animals (*n* = 3–4) needed for *in vitro* analyses. The probability that an animal dies of causes unrelated to the experiment in our longest group was approximately 10% based on previous experience. We, therefore, arrived at a preliminary calculation of 10 animals in this study. All results are presented as mean ± SEM. Data were analyzed using GraphPad Prism 8 (GraphPad Software, San Diego, CA, USA, www.graphpad.com). Statistical analyses were performed using either paired Student's *t*-test, or one- or two-way analysis of variance followed by Tukey's *post hoc* test for multiple comparisons. A *P* value of < 0.05 was considered to be statistically significant.

Results

Functional recovery and animal loss following nerve transection and gap-grafting: effects of 4-AP

We have consistently demonstrated a beneficial effect of 4-AP on the functional recovery after sciatic nerve crush injury in mice (Tseng et al., 2016; Clark et al., 2019; Noble et al., 2019; Yue et al., 2019; Hsu et al., 2020). Here we sought to explore the long-term effects of systemic 4-AP treatment on post-injury functional recovery in three severe peripheral nerve injury models: (1) stepwise nerve transection with gluing (STG); (2) 7 mm irreparable nerve gap (G-7/0), and (3) 7 mm isografting in 5 mm gap (G-5/7) (**Figure 1A–C**). As described recently (Lee et al., 2020), in STG method as shown in **Figure 1A**, the nerve was first transected to 80% of its width to prevent gap formation between the cut ends, then 10 µL of fibrin glue was applied around the transection site and the nerve was completely transected before complete clotting of fibrin glue. In the graded nerve gap and grafting model (**Figure 1B** and **C**), in mouse #1, a large gap was created by dissecting 7 mm (G-7/0) of the right sciatic nerve section. The proximal stump of the sciatic nerve was buried underneath the muscle with 10 µL of fibrin glue. Then, in mouse #2, a medium gap was created by dissecting 5 mm of the right sciatic nerve section, and the 7 mm dissected nerve section from mouse #1 was grafted and kept in good alignment with fibrin glue at both ends (G-5/7).

SFI is the most frequently used regenerative outcome measure after sciatic nerve injury and uses ink prints of the hind paw on paper to measure the distances of the paw print length, toe spread, and intermediate toe spread (Wood et al., 2011). The measures from these footprints are used to calculate SFI, as described in detail in the Methods section. **Figure 3A** shows that average post-injury SFI values in the saline STG model were significantly greater than the G-7/0 model and it was ~40–50% of the pre-injury baseline value. The SFI in the G-5/7 model demonstrated an erratic recovery which was variable across mice in the group. The SFI in G-7/0 remained persistently worse and further degraded over time compared with STG and G-5/7 models, and this worsening in walking function was consistent across mice in the G-7/0 group. Of note, we had 10 mice in each injury model, only one mouse in the G-7/0 4-AP group died after 8 weeks of surgery. In the STG model, two mice in both saline and 4-AP groups failed to produce measurable footprints after 4 weeks of surgery. In the G-5/7 model, nearly half of the mice in saline and 4-AP groups were unable to walk properly 4 weeks after surgery, that is, to walk in a way that produces measurable footprints. Footprints from these mice were not used in the data analysis because they were not quantifiable. While mice in the G-5/7 model did not show any SFI recovery compared with the STG model until 4 weeks post-surgery, SFI recovery between STG and G-5/7 was comparable after 6 weeks of surgery. In contrast, all mice in the G-7/0 model were able to produce quantifiable footprints until the end of the 12-week experimental period, although the footprints were persistently abnormal. Taken together, these findings demonstrate that regardless of nerve transection, gap-grafting, and irreparable gap, 4-AP treatment has no beneficial effect on the SFI recovery in any model (**Figure 3B–D**).

Visualization of peripheral nerve regeneration after nerve transection and gap-grafting

To examine the histology of the regenerating nerve after 12 weeks of surgery, we performed immunofluorescence staining of the whole nerve stained with NF-H to label neurofilament, CD31 to label blood vessels, MP0 to label myelin, and DAPI to label nuclei. We first compared the STG model treated with saline and 4-AP (**Figure 4**). **Figure 4** shows representative whole-mount immunofluorescence images of left (uninjured; A) and right (injured) sciatic nerves in saline (injured-saline; B) and 4-AP (injured-4-AP; C) groups of the STG model stained with NF-H, CD31, MP0, and DAPI. Uninjured nerve displays normal nerve architecture with uniform neurofilaments (NF-H), blood vessels (CD31), myelination (MP0), DAPI, and merged staining over the entire length. In contrast, peri-injury and distal ends of the injured nerve in both saline and 4-AP groups are markedly different with misdirected neurofilaments and branched blood vessels. We did not observe any noticeable effect of 4-AP on the regenerating nerve after STG surgery.

We next examined the G-5/7 model treated with saline and 4-AP for nerve histology (**Figure 5**). **Figure 5** shows representative whole-mount immunofluorescence images of left (uninjured; A) and right (injured) sciatic nerves in saline (injured-saline; B) and 4-AP (injured-4-AP; C) groups of the G-5/7 model stained with NF-H, CD31, MP0, and DAPI. While the uninjured nerve demonstrates normal nerve architecture with uniform NF-H, MP0, and DAPI and merged staining over the entire length, the isografted nerve (G-5/7) in both saline and 4-AP groups was strikingly different from the uninjured nerve with bulging at the peri-isograft areas, aberrant distribution of neurofilaments, and disruption of myelination. The magnified images of an isografted nerve (G-5/7 saline) in **Figure 6** shows markedly distorted and haphazardly arranged neurofilament-stained regenerating axons with myelin breakdown. Similar to the STG model we did not observe any noticeable effect of 4-AP on the regenerating nerve in the G-5/7 model. In the G-7/0 model, there was no nerve to examine because it was dissected out for isografting and the proximal end was buried inside the adjacent muscle.

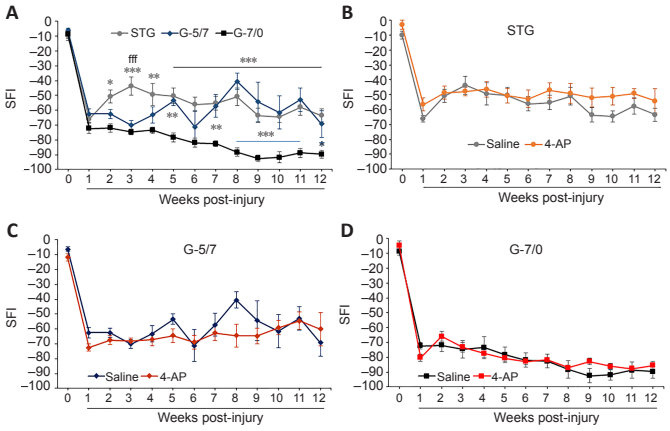

Figure 3 | Functional recovery as SFI from baseline in saline and 4-AP treatment groups of STG, G-5/7, and G-7/0 models.
An irreparable gap (G-7/0) caused persistently worse and degrading SFI throughout the experimental protocol compared with STG and G-5/7 models (A). 4-AP treatment did not affect SFI recovery in any model (B–D). Data are expressed as the mean ± SEM, and data at each point came from 5–10 mice. Pre-injury baseline SFI value is shown at 0 time point of the *x*-axis. **P* < 0.05, ***P* < 0.01, ****P* < 0.001, STG or G-5/7 *vs*. G-7/0; fff*P* < 0.001, STG *vs*. G-5/7 (two-way analysis of variance followed by Tukey's *post hoc* test). 4-AP: 4-Aminopyridine; G-5/7: 5 mm gap and 7 mm nerve grafting; G-7/0: 7 mm permanent nerve gap; SFI: sciatic functional index; STG: stepwise transection and fibrin glue.

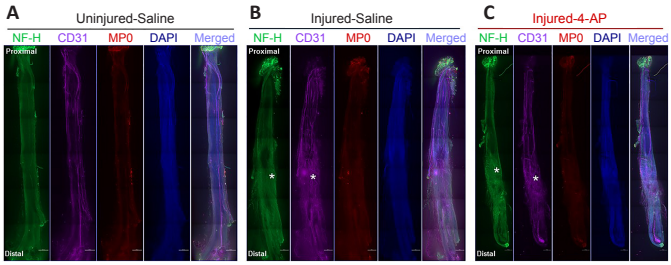

Figure 4 | Whole-mount immunofluorescence imaging of the sciatic nerve for neurofilaments, blood vessels, and myelin proteins.
Representative compact images, from an uninjured left sciatic nerve (A) and glue-repaired transected right sciatic nerves of STG model with saline (B) or 4-AP treatment (C), to show the orientation and distribution of neurofilaments (NF-H, green), blood vessels (CD31, purple), myelination (MP0, red), and DAPI (blue), as well as the merged view from proximal to distal end of the nerve. White asterisks indicate misdirectional neurofilaments and branched blood vessels extending from the peri-injury area to the distal end of the nerve. Scale bars: 500 µm, original magnification, 5×. Each image is representative of at least four immunostained whole nerves from four different mice. 4-AP: 4-Aminopyridine; DAPI: 4′,6-diamidino-2-phenylindole; STG: stepwise transection and fibrin glue.

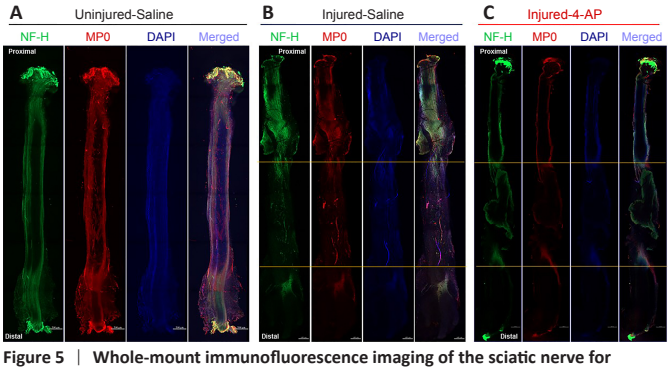

Figure 5 | Whole-mount immunofluorescence imaging of the sciatic nerve for neurofilaments, blood vessels, and myelin proteins.
Representative compact images, from an uninjured left sciatic nerve (A) and isografted right sciatic nerves of G-5/7 model with saline (B) or 4-AP treatment (C), to show the orientation and distribution of neurofilaments (NF-H, green), myelination (MP0, red), and DAPI (blue), as well as the merged view at different zones of the nerve. Isogrfated nerve and peri-isograft areas in between two yellow horizontal lines display distorted and aberrant distribution of neurofilaments and myelin. Scale bars: 500 µm; original magnification, 5×. Each image is representative of at least four immunostained whole nerves from four different mice. 4-AP: 4-Aminopyridine; DAPI: 4′,6-diamidino-2-phenylindole; G-5/7: 5 mm gap and 7 mm nerve grafting.

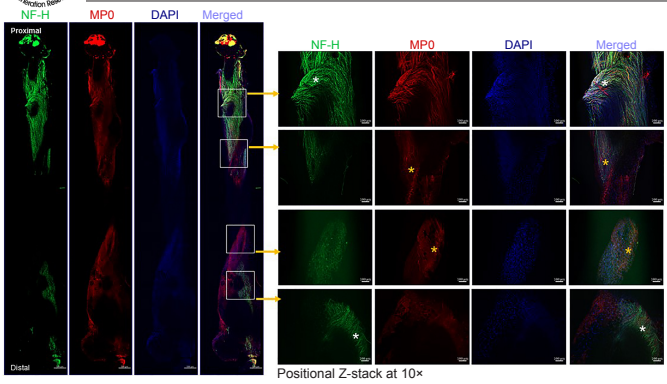

Figure 6 | Whole-mount immunofluorescence imaging of the sciatic nerve for neurofilaments, blood vessels, and myelin proteins.
Representative (5×) and positional Z-stack compact images at 10× from an isografted right sciatic nerve (G-5/7) with saline treatment to show the orientation and distribution of neurofilaments (NF-H, green), myelination (MP0, red), and DAPI (blue), as well as the merged view at different zones of the nerve. White asterisks indicate an abundance of aberrant neurofilaments, and yellow asterisks indicate myelin disruption. Scale bars: 100 µm for 10× images and 100 µm for 5× images. Each image is representative of at least four immunostained whole nerves from four different mice. DAPI: 4′,6-Diamidino-2-phenylindole; G-5/7: 5 mm gap and 7 mm nerve grafting.

Muscle atrophy after nerve transection and gap-grafting: effects of 4-AP

Denervation causes rapid muscle atrophy within weeks of the injury (Lien et al., 2008; Wu et al., 2014) and we have recently demonstrated a significant beneficial effect of 4-AP on neurogenic muscle atrophy, muscle regenerating stem cell numbers, and *ex vivo* muscle force after sciatic nerve crush injury in mice (Yue et al., 2019). Here we wanted to investigate the long-term effects of 4-AP treatment on neurogenic muscle atrophy in three severe peripheral nerve injury models: STG, G-5/7, and G-7/0. To evaluate the extent of denervation muscle atrophy and the effect of 4-AP: First, we checked the changes in muscle mass and then we performed the histological and histomorphometric analysis of the muscles to determine CSA and MFD in both left tibialis anterior (LTA) and right tibialis anterior (RTA) muscles after 12 weeks of surgery. Of note, while muscle wet weight is a gross measurement of whole muscle mass and is used as an index of muscle innervation, CSA and MFD represent muscle atrophy at a single muscle fiber level and are used to assess muscle contractile properties. **Table 1** shows the absolute values and **Figure 7** shows quantitative RTA muscle mass (A), CSA (B) and MFD (C) normalized to LTA (contralateral healthy left limb). While muscle mass in the saline and 4-AP groups of G-7/0 was significantly reduced compared with STG and G-5/7, 4-AP treatment attenuated muscle loss significantly in G-7/0. Similarly, while CSA and MFD in the saline G-7/0 were significantly smaller compared with STG and G-5/7, 4-AP treatment significantly improved CSA and MFD in G-7/0 such that the data in the 4-AP-treated animals of G-7/0 group were comparable to STG and G-5/7 models. These findings demonstrate that 4-AP treatment can reduce muscle atrophy with marked increases in both CSA and MFD only in the irreparable nerve gap model (G-7/0) indicating a muscle protective and perhaps muscle force enhancing effect of 4-AP in long-term denervation.

Table 1 | Average muscle mass, CSA, and MFD after 12 weeks of nerve transection (STG), isografting (G-5/7), and irreparable gap (G-7/0)

	LTA	RTA	*n*	*P*-value
Muscle mass (mg)				
STG: Saline	58.34±1.77	51.81±2.01	10	$P < 0.05$, Saline: STG LTA *vs.* RTA
STG: 4-AP	56.30±1.92	50.53±1.67	10	$P < 0.05$, 4-AP: STG LTA *vs.* RTA
G-5/7: Saline	63.01±1.25	50.41±0.70	10	$P < 0.001$, Saline: G-5/7 LTA *vs.* RTA
G-5/7: 4-AP	62.07±1.68	51.05±0.67	10	$P < 0.001$, 4-AP: G-5/7 LTA *vs.* RTA
G-7/0: Saline	66.98±2.80	15.93±0.51	10	$P < 0.001$, Saline: G-7/0 LTA *vs.* RTA
G-7/0: 4-AP	59.91±1.67	16.69±1.07	9	$P < 0.001$, 4-AP: G-7/0 LTA *vs.* RTA
CSA (µm²)				
STG: Saline	1887.11±7.43	1538.23±13.97	4	$P < 0.05$, Saline: STG LTA *vs.* G-5/7 LTA
STG: 4-AP	1759.58±6.20	1670.14±7.04	4	$P < 0.01$, 4-AP: STG LTA *vs.* G-7/0 LTA
G-5/7: Saline	2236.25±8.02	2035.16±12.80	4	$P < 0.01$, Saline: G-5/7 RTA *vs.* G-7/0 RTA
G-5/7: 4-AP	2358.45±9.76	2032.46±14.52	4	$P < 0.01$, 4-AP: G-5/7 LTA *vs.* STG LTA
G-7/0: Saline	1946.79±13.16	1047.52±4.03	4	$P < 0.01$, Saline: G-7/0 RTA *vs.* LTA
G-7/0: 4-AP	2467.26±11.76	1918.08±29.04	4	
MFD (µm)				
STG: Saline	43.68±0.10	41.72±0.14	4	$P < 0.01$, Saline: STG RTA *vs.* G-7/0 RTA
STG: 4-AP	42.89±0.08	42.75±0.07	4	$P < 0.05$, 4-AP: STG LTA *vs.* G-7/0 LTA
G-5/7: Saline	45.79±0.07	44.92±0.15	4	$P < 0.01$, Saline: G-5/7 RTA *vs.* G-7/0 RTA
G-5/7: 4-AP	47.61±0.09	44.66±0.14	4	$P < 0.05$, 4-AP: G-5/7 LTA *vs.* STG LTA
G-7/0: Saline	45.53±0.04	31.91±0.04	4	$P < 0.01$, Saline: G-7/0 RTA *vs.* LTA
G-7/0: 4-AP	48.89±0.11	42.20±0.28	4	$P < 0.05$, G-7/0: Saline RTA *vs.* 4-AP RTA

CSA: Cross-sectional area; LTA: left tibialis anterior; MFD: minimal Feret's diameter; RTA: right tibialis anterior; STG: stepwise transection and fibrin glue.

Finally, we determined the muscle fiber distribution ratio in the G-7/0 group after 12 weeks of surgery (**Figure 8**) based on the MFD data to evaluate the impact of 4-AP treatment on the frequency of different muscle fiber sizes. In the saline group (**Figure 8A**), while most of the LTA muscle fibers (uninjured) were distributed in the range 40–60 µm diameters, the RTA muscle fibers (injured) revealed a leftward shift in fiber distribution with a predominance of smaller fibers in the range 25–40 µm diameters. In contrast, in the 4-AP treatment group (**Figure 8B**), muscle fiber distribution frequency between LTA (uninjured) and RTA (injured) muscles was comparable: LTA muscle fibers were distributed in the range 40–60 µm diameters and RTA muscle fibers were distributed in the range 35–55 µm diameters, indicating an optimal distribution ratio. **Figure 8C** comparing the fiber distribution frequency in the injured RTA muscle of saline and 4-AP groups clearly demonstrates that 4-AP treatment was able to preserve most muscle fiber size-frequency within 35–55 µm ranges compared with the saline group at 25–40 µm ranges. Taken together, improved muscle mass, CSA, MFD, and muscle fiber distribution in the G-7/0 model provides significant evidence to suggest that 4-AP treatment at least has some beneficial effect on long-term neurogenic muscle atrophy.

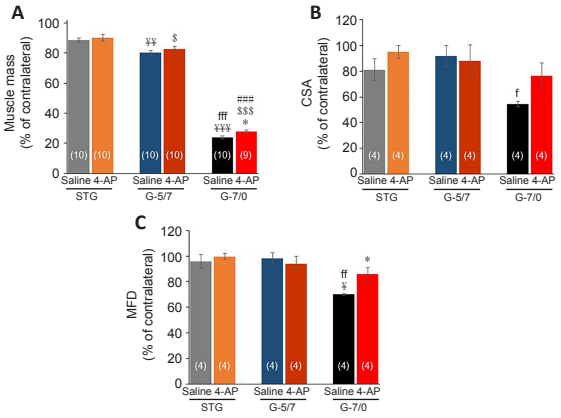

Figure 7 | Effects of STG, G-5/7, and G-7/0 on TA muscle mass and quantitative measurements of the muscle fibers.
(A) Right TA (RTA) muscle mass as % of contralateral (left) side, n = 9–10/group (shown at each bar); (B) cross-sectional area (CSA) of RTA muscle as % of contralateral (left) side, n = 4/group; and (C) minimum Feret's diameter (MFD) of RTA muscle as % of contralateral (left) side. Data are expressed as the mean ± SEM. Data derived from three random microscopic fields from each muscle, and four muscle sections from different mice were used (n = 4/group). ¥P < 0.05, ¥¥P < 0.01, ¥¥¥P < 0.001, *vs.* STG saline; fP < 0.05, ff$P$ < 0.01, fff$P$ < 0.001, *vs.* G-5/7 saline; P < 0.05, $$$P$ < 0.001, *vs.* STG 4-AP; ###P < 0.001, *vs.* G-5/7 4-AP; *P < 0.05, *vs.* G-7/0 saline (two-way analysis of variance followed by Tukey's *post hoc* test). G-5/7: 5 mm gap and 7 mm nerve grafting; G-7/0: 7 mm permanent nerve gap; SFI: sciatic functional index; STG: stepwise transection and fibrin glue; TA: tibialis anterior.

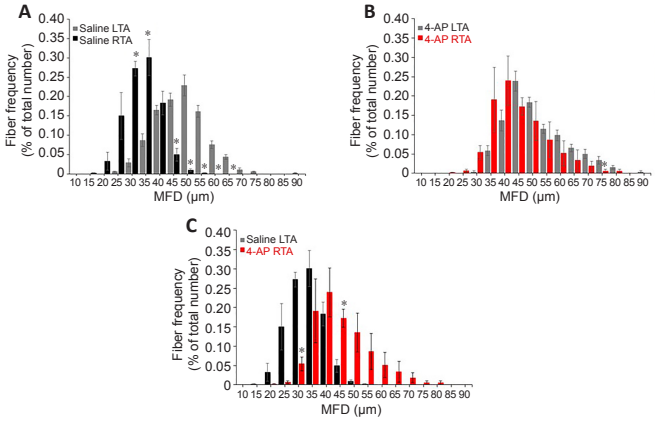

Figure 8 | Effect of G-7/0 models on muscle fiber distribution.
Quantitative muscle fiber size distribution from the minimal Feret's diameter value (µm) in each group as a percentage of total fiber number. (A) Fiber distribution between LTA and RTA muscles in the saline group. (B) Fiber distribution between LTA and RTA muscles in the 4-AP group. (C) Fiber distribution between RTA muscles in the saline and 4-AP groups. Data are expressed as the mean ± SEM. Data derived from three random microscopic fields from each muscle, and 4 muscle sections from different mice were used (n = 4/group); *P < 0.05, respective RTA *vs.* LTA in A and B; *P < 0.05, saline RTA *vs.* 4-AP RTA in C (two-way analysis of variance followed by Tukey's *post hoc* test). G-5/7: 5 mm gap and 7 mm nerve grafting; G-7/0: 7 mm permanent nerve gap; LTA: left tibialis anterior; RTA: right tibialis anterior; SFI: sciatic functional index; STG: stepwise transection and fibrin glue.

Discussion

The functional outcomes following advanced microsurgical peripheral nerve repair and reconstruction are disappointing and unpredictable, particularly when PNI results in large gaps between the severed nerve ends. In our recent short-term study with a novel nerve transection and repair model in mice (Lee et al., 2020), we reported that fibrin glue can replace sutures with favorable findings on the nerves and muscles. While we demonstrated that systemic 4-AP treatment improves functional recovery and neurogenic muscle atrophy after sciatic nerve crush injury in mice (Tseng et al., 2016; Clark et al., 2019; Noble et al., 2019; Hsu et al., 2020), nerve gap filled with collagen gel mixed with 4-AP had no effect on the axonal counts after 6 weeks of sciatic nerve transection injury in rats (Harman et al., 1991) and sustained release of 4-AP from biopolymer-nanotube nerve guidance drug-conduit showed similar functional recovery and regenerative efficacy as compared with autograft alone after eight weeks of sciatic nerve transection injury in rats (Manoukian et al., 2021). Therefore, we designed this study to evaluate the long-term outcomes of novel nerve transection and syngeneic nerve grafting with gluing and the effect of 4-AP. Overall, we found that the functional recovery, nerve morphology, and muscle atrophy after PNI and repair are directly related to the size/severity of the intervening nerve gap, and 4-AP exerts differential effects on the functional recovery and muscle atrophy: No effect on post-injury functional recovery in STG, G-5/7, and G-7/0 models, but significant muscle atrophy-mitigating effects in irreparable nerve gap model (G-7/0). Since fibrin glue is widely used for nerve transection, nerve graft, or nerve transfer repairs (Martins et al., 2005; Sameem et al., 2011; Spotnitz, 2014; Koulaxouzidis et al., 2015; Benfield et al., 2021), these pre-clinical mouse models of nerve transection and nerve gap-grafting could be useful tools to investigate morphological, functional, cellular, and molecular characteristics of PNI for novel therapeutic strategies.

While there are several microsurgical repair options, such as direct repair, nerve grafting, nerve transfer, nerve transplant, or nerve conduits, the gold standard of nerve repair is end-to-end neurorrhaphy if the nerve gap is less than 1 cm (Siemionow and Brzezicki, 2009; Evans, 2001; Isaacs, 2013). For larger nerve gaps (> 1 cm), the gold standard for the treatment of nerve gaps is autologous nerve grafting which is primarily a sensory nerve in patients (Sachanandani et al., 2014; Bassilios Habre et al., 2018). Currently, there is limited information on how each method of nerve repair with glue might influence the long-term functional outcome and morphological aspect of nerve regeneration (Koulaxouzidis et al., 2015). Macroscopically, we observed that the nerves in STG and G-5/7 were in well-connected condition and had good continuity with a bulge at the repair site, and there was no dehiscence 12 weeks after surgery. Consistent with our recent short-term study (Lee et al., 2020), we observed comparable long-term functional recovery and qualitative morphological changes with whole-mount nerve imaging after STG. However, even with an identical syngeneic nerve grafting, we observed erratic and poor functional recovery in the G-5/7 model associated with morphologically distorted nerve and an abundance of misdirected nerve fibers at the repaired sites when compared with the whole mount nerve images of STG. Although the mechanisms of these findings with isografting were not investigated in this study, the pathophysiological and nerve regeneration processes associated with nerve grafting could be quite different, more complex, and multifactorial compared to STG because nerve grafting has two repair sites compared to single repair site with STG. This can lead to slow staggered regeneration of axons across the repair sites before entering the distal nerve stump. Moreover, isograft may also have donor site mismatch, limited blood supply, scarring, and secondary removal of degenerated axons and myelin by the host from the graft itself (Sachanandani et al., 2014; Bassilios Habre et al., 2018). In contrast to STG and G-5/7, the increasingly degraded functional deficit over time with G-7/0 reflected the extreme feature of long-term denervation.

Denervation muscle atrophy occurs very rapidly following a nerve injury and we found that muscle atrophy in the injured hindlimb after 12 weeks of surgery progressively increased with injury severity from STG to G-7/0 (STG < G-5/7 < G-7/0). The denervated muscle is characterized by reduced muscle mass, decreased CSA, increased connective tissue, and altered muscle fiber distribution (Engel and Stonnington, 1974; Dedkov et al., 2003; Lien et al., 2008; Sobotka and Mu, 2015). Muscle wet weight is used to evaluate muscle innervation (Liu et al., 1999; Sobotka and Mu, 2015), thus decreasing muscle mass with increasing gap length in this study suggests poor muscle innervation with increasing injury severity. The severity of muscle atrophy in the G-7/0 model also suggests that reapproximation of severed nerve ends with fibrin glue or isografting is important for muscle mass preservation. CSA is commonly used for single muscle fiber size, but values can be distorted by the orientation of the muscle sectioning angle. To verify CSA, we also used MFD which provides a better estimate of muscle fiber diameter because it is least influenced by the sectioning angle (Briguet et al., 2004). We found that both CSA and MFD in the saline group of STG and G-5/7 were comparable, while they were significantly smaller in G-7/0. Taken together, these findings confirm that repair of the severed nerve is critical to retard denervation muscle atrophy.

Our findings in this study with 4-AP on sciatic nerve transection, gap, and grafting were mixed and somewhat interesting. While 4-AP treatment had no effect on the functional recovery in STG, G-5/7, and G-7/0 models, or on the muscle atrophy in STG and G-5/7 models, 4-AP significantly reduced muscle atrophy in the G-7/0 model and it was associated with markedly improved CSA and MFD. Importantly, the 4-AP treatment improved muscle fiber size distribution in the injured hindlimb by shifting it from lower (leftward) to higher (rightward) size ranges. It is widely believed that when muscle remains denervated for a long time, its function cannot be recovered because regenerating nerve fibers cannot reinnervate the terminally atrophied target muscles (Engel and Stonnington, 1974; Lien et al., 2008). Although these findings clearly indicate a direct effect of 4-AP on muscle fiber size and mass recovery in an exclusively denervated muscle, the mechanisms of this recovery and the force-generating capacity of this muscle remain to be explored. It should also be noted that our study has several limitations, specifically the absence of nerve fiber quantification, neuromuscular junction structure, muscle force, and electrophysiological data, which might better reveal the functional recovery and muscle atrophy.

It is impossible with animal studies to exactly mimic the pathophysiological changes seen with nerve transection, gap, and grafting in humans. However, using fibrin glue in nerve transection repair and grafting in mice, we were able to show that increased nerve gap length and injury severity is associated with decreased functional recovery, aberrant nerve fiber regeneration, and increased muscle atrophy. Our interesting pre-clinical findings with 4-AP on long-term muscle atrophy in irreparable nerve gaps have tremendous clinical implications because it opens up a novel avenue for further investigations of 4-AP in diverse pre-clinical disease models of muscle atrophy in larger animals for better clinical extrapolation and comparison.

Author contributions: *Concept and design of the study, surgery and tissue harvesting, data acquisition, and final approval: JIL. Design of the study, tissue harvesting, data acquisition and analysis, organization and interpretation, writing initial draft, compiling, revising and editing the draft with intellectual content, and final approval: MAHT. Data analysis, organization and interpretation, and final approval: ZK. Tissue harvesting, data acquisition, and final approval: AAG. Tissue harvesting, data acquisition, and final approval: PKG. Data acquisition and final approval: JMG, DLW. Data analysis and final approval: KMM, GDW, JPH. Concept and design of the study, funding acquisition, data interpretation, revising and editing the draft with intellectual content, and final approval: JCE.*

Conflicts of interest: *None declared.*

Availability of data and materials: *All data generated or analyzed during this study are included in this published article and its supplementary information files.*

Open peer reviewers: *David Brogan, Washington University in St Louis, USA; Carol Schuurmans, Sunnybrook Research Institute, Canada.*

Additional files:

Additional file 1: *Supplemental methods.*

Additional file 2: *Open peer review reports 1 and 2.*

Additional Figure 1: *Dose-escalating effect of 4-AP on the functional recovery as sciatic function index in saline and 4-AP treatment groups before (baseline) and after severe sciatic nerve crush injury (on post-injury days 3, 7, 14, and 21).*

References

Bassilios Habre S, Bond G, Jing XL, Kostopoulos E, Wallace RD, Konofaos P (2018) The surgical management of nerve gaps: present and future. Ann Plast Surg 80:252-261.

Benfield C, Isaacs J, Mallu S, Kurtz C, Smith M (2021) Comparison of nylon suture versus 2 fibrin glue products for delayed nerve coaptation in an animal model. J Hand Surg Am 46:119-125.

Briguet A, Courdier-Fruh I, Foster M, Meier T, Magyar JP (2004) Histological parameters for the quantitative assessment of muscular dystrophy in the mdx-mouse. Neuromuscul Disord 14:675-682.

Campbell WW (2008) Evaluation and management of peripheral nerve injury. Clin Neurophysiol 119:1951-1965.

Chan KM, Gordon T, Zochodne DW, Power HA (2014) Improving peripheral nerve regeneration: from molecular mechanisms to potential therapeutic targets. Exp Neurol 261:826-835.

Clark AR, Hsu CG, Talukder MAH, Noble M, Elfar JC (2019) Transdermal delivery of 4-aminopyridine accelerates motor functional recovery and improves nerve morphology following sciatic nerve crush injury in mice. Neural Regen Res 15:136-144.

Day CS, Riano F, Tomaino MM, Buranatanitkit B, Somogyi G, Sotereanos D, Huard J (2001) Growth factor may decrease muscle atrophy secondary to denervation. J Reconstr Microsurg 17:51-57.

Dedkov EI, Borisov AB, Carlson BM (2003) Dynamics of postdenervation atrophy of young and old skeletal muscles: differential responses of fiber types and muscle types. J Gerontol A Biol Sci Med Sci 58:984-991.

Engel AG, Stonnington HH (1974) Trophic functions of the neuron. II. Denervation and regulation of muscle. Morphological effects of denervation of muscle. A quantitative ultrastructural study. Ann N Y Acad Sci 228:68-88.

Evans GR (2001) Peripheral nerve injury: a review and approach to tissue engineered constructs. Anat Rec 263:396-404.

Faroni A, Mobasseri SA, Kingham PJ, Reid AJ (2015) Peripheral nerve regeneration: experimental strategies and future perspectives. Adv Drug Deliv Rev 82-83:160-167.

Fernandez L, Komatsu DE, Gurevich M, Hurst LC (2018) Emerging strategies on adjuvant therapies for nerve recovery. J Hand Surg Am 43:368-373.

Foster CH, Karsy M, Jensen MR, Guan J, Eli I, Mahan MA (2019) Trends and cost-analysis of lower extremity nerve injury using the national inpatient sample. Neurosurgery 85:250-256.

Harman K, Katnick J, Lim R, Zaheer A, de la Torre JC (1991) Glia maturation factor beta stimulates axon regeneration in transected rat sciatic nerve. Brain Res 564:332-335.

Hsu CG, Talukder MAH, Yue L, Turpin LC, Noble M, Elfar JC (2020) Human equivalent dose of oral 4-aminopyridine differentiates nerve crush injury from transection injury and improves post-injury function in mice. Neural Regen Res 15:2098-2107.

Hussain G, Wang J, Rasul A, Anwar H, Qasim M, Zafar S, Aziz N, Razzaq A, Hussain R, de Aguilar JG, Sun T (2020) Current status of therapeutic approaches against peripheral nerve injuries: a detailed story from injury to recovery. Int J Biol Sci 16:116-134.

Isaacs J (2013) Major peripheral nerve injuries. Hand Clin 29:371-382.

Karsy M, Watkins R, Jensen MR, Guan J, Brock AA, Mahan MA (2019) Trends and cost analysis of upper extremity nerve injury using the national (nationwide) inpatient sample. World Neurosurg 123:e488-500.

Koulaxouzidis G, Reim G, Witzel C (2015) Fibrin glue repair leads to enhanced axonal elongation during early peripheral nerve regeneration in an in vivo mouse model. Neural Regen Res 10:1166-1171.

Lee JI, Gurjar AA, Talukder MAH, Rodenhouse A, Manto K, O'Brien M, Govindappa PK, Elfar JC (2020) A novel nerve transection and repair method in mice: histomorphometric analysis of nerves, blood vessels, and muscles with functional recovery. Sci Rep 10:21637.

Lien SC, Cederna PS, Kuzon WM (2008) Optimizing skeletal muscle reinnervation with nerve transfer. Hand Clin 24:445-454, vii.

Liu K, Chen LE, Seaber AV, Goldner RV, Urbaniak JR (1999) Motor functional and morphological findings following end-to-side neurorrhaphy in the rat model. J Orthop Res 17:293-300.

Manoukian OS, Rudraiah S, Arul MR, Bartley JM, Baker JT, Yu X, Kumbar SG (2021) Biopolymer-nanotube nerve guidance conduit drug delivery for peripheral nerve regeneration: In vivo structural and functional assessment. Bioact Mater 6:2881-2893.

Martínez de Albornoz P, Delgado PJ, Forriol F, Maffulli N (2011) Non-surgical therapies for peripheral nerve injury. Br Med Bull 100:73-100.

Martins RS, Siqueira MG, Da Silva CF, Plese JP (2005) Overall assessment of regeneration in peripheral nerve lesion repair using fibrin glue, suture, or a combination of the 2 techniques in a rat model. Which is the ideal choice? Surg Neurol 64 Suppl 1:S1:10-16.

Menorca RM, Fussell TS, Elfar JC (2013) Nerve physiology: mechanisms of injury and recovery. Hand Clin 29:317-330.

Modrak M, Talukder MAH, Gurgenashvili K, Noble M, Elfar JC (2020) Peripheral nerve injury and myelination: Potential therapeutic strategies. J Neurosci Res 98:780-795.

Nair AB, Jacob S (2016) A simple practice guide for dose conversion between animals and human. J Basic Clin Pharm 7:27-31.

Noble J, Munro CA, Prasad VS, Midha R (1998) Analysis of upper and lower extremity peripheral nerve injuries in a population of patients with multiple injuries. J Trauma 45:116-122.

Noble M, Tseng KC, Li H, Elfar JC (2019) 4-Aminopyridine as a single agent diagnostic and treatment for severe nerve crush injury. Mil Med 184:379-385.

Robinson LR (2000) Traumatic injury to peripheral nerves. Muscle Nerve 23:863-873.

Robinson LR (2004) Traumatic injury to peripheral nerves. Suppl Clin Neurophysiol 57:173-186.

Sachanandani NF, Pothula A, Tung TH (2014) Nerve gaps. Plast Reconstr Surg 133:313-319.

Sameem M, Wood TJ, Bain JR (2011) A systematic review on the use of fibrin glue for peripheral nerve repair. Plast Reconstr Surg 127:2381-2390.

Schneider CA, Rasband WS, Eliceiri KW (2012) NIH Image to ImageJ: 25 years of image analysis. Nat Methods 9:671-675.

Siemionow M, Brzezicki G (2009) Chapter 8: Current techniques and concepts in peripheral nerve repair. Int Rev Neurobiol 87:141-172.

Sobotka S, Mu L (2015) Muscle reinnervation with nerve-muscle-endplate band grafting technique: correlation between force recovery and axonal regeneration. J Surg Res 195:144-151.

Spotnitz WD (2014) Fibrin sealant: the only approved hemostat, sealant, and adhesive-a laboratory and clinical perspective. ISRN Surg 2014:203943.

Tseng KC, Li H, Clark A, Sundem L, Zuscik M, Noble M, Elfar J (2016) 4-Aminopyridine promotes functional recovery and remyelination in acute peripheral nerve injury. EMBO Mol Med 8:1409-1420.

Udina E, Cobianchi S, Allodi I, Navarro X (2011) Effects of activity-dependent strategies on regeneration and plasticity after peripheral nerve injuries. Ann Anat 193:347-353.

Varejão AS, Meek MF, Ferreira AJ, Patrício JA, Cabrita AM (2001) Functional evaluation of peripheral nerve regeneration in the rat: walking track analysis. J Neurosci Methods 108:1-9.

Wong A, Pomerantz JH (2019) The role of muscle stem cells in regeneration and recovery after denervation: a review. Plast Reconstr Surg 143:779-788.

Wood MD, Kemp SW, Weber C, Borschel GH, Gordon T (2011) Outcome measures of peripheral nerve regeneration. Ann Anat 193:321-333.

Wu P, Chawla A, Spinner RJ, Yu C, Yaszemski MJ, Windebank AJ, Wang H (2014) Key changes in denervated muscles and their impact on regeneration and reinnervation. Neural Regen Res 9:1796-1809.

Yue L, Talukder MAH, Gurjar A, Lee JI, Noble M, Dirksen RT, Chakkalakal J, Elfar JC (2019) 4-Aminopyridine attenuates muscle atrophy after sciatic nerve crush injury in mice. Muscle Nerve 60:192-201.

Zochodne DW (2012) The challenges and beauty of peripheral nerve regrowth. J Peripher Nerv Syst 17:1-18.

P-Reviewers: Brogan D, Schuurmans C; C-Editors: Zhao M, Liu WJ; S-Editor: Li CH; L-Editors: Li CH, Song LP; T-Editor: Jia Y

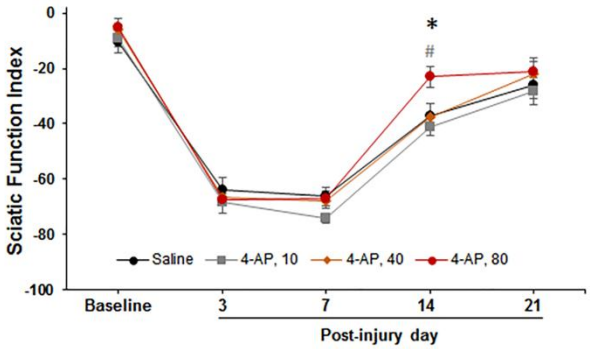

Additional Figure 1 Dose-escalating effect of 4-AP on the functional recovery as sciatic function index in saline and 4-AP treatment groups before (baseline) and after severe sciatic nerve crush injury (on post-injury days 3, 7, 14, and 21).

4-AP was given intraperitoneally daily as 10, 40, and 80 μg per 20 g mouse. Data are expressed as the mean ± SEM, and data at each point is derived from 9 mice. *$P < 0.05$, vs. saline; $^{\#}P < 0.05$, vs. 4-AP 10 μg (two-way analysis of variance followed by Tukey's post hoc test for multiple comparisons). 4-AP: 4-Aminopyridine.